Published in final edited form as:
Eur J Nucl Med Mol Imaging. 2011 July ; 38(7): 1335–1343. doi:10.1007/s00259-011-1765-5.

Positron emission tomography imaging of CD105 expression during tumour angiogenesis

Hao Hong[1,6], **Yunan Yang**[1,5,6], **Yin Zhang**[2,6], **Jonathan W. Engle**[2], **Todd E. Barnhart**[2], **Robert J. Nickles**[2], **Bryan R. Leigh**[3], and **Weibo Cai**[1,2,4,*]

[1]Department of Radiology, University of Wisconsin - Madison, Madison, WI, USA

[2]Department of Medical Physics, University of Wisconsin - Madison, Madison, WI, USA

[3]TRACON Pharmaceuticals, Inc., San Diego, CA, USA

[4]University of Wisconsin Carbone Cancer Center, Madison, WI, USA

[5]Department of Ultrasound, Xinqiao Hospital, Third Military Medical University, Chongqing 400037, P. R. China

Abstract

Purpose—Overexpression of CD105 (endoglin) correlates with poor prognosis in many solid tumour types. Tumour microvessel density (MVD) assessed by CD105 staining is the current gold standard for evaluating tumour angiogenesis in the clinic. The goal of this study was to develop a positron emission tomography (PET) tracer for imaging CD105 expression.

Methods—TRC105, a chimeric anti-CD105 monoclonal antibody, was conjugated to DOTA and labeled with ^{64}Cu. FACS analysis and microscopy studies were performed to compare the CD105 binding affinity of TRC105 and DOTA-TRC105. PET imaging, biodistribution, blocking, and ex vivo histology studies were performed on 4T1 murine breast tumour-bearing mice to evaluate the ability of ^{64}Cu-DOTA-TRC105 to target tumour angiogenesis. Another chimeric antibody, cetuximab, was used as an isotype-matched control.

Results—FACS analysis of HUVECs revealed no difference in CD105 binding affinity between TRC105 and DOTA-TRC105, which was further validated by fluorescence microscopy. ^{64}Cu-labeling was achieved with high yield and specific activity. Serial PET imaging revealed that the 4T1 tumour uptake of the tracer was 8.0 ± 0.5, 10.4 ± 2.8, and 9.7 ± 1.8 %ID/g at 4, 24, and 48 h post-injection respectively (n = 3), higher than most organs at late time points which provided excellent tumour contrast. Biodistribution data as measured by gamma counting were consistent with the PET findings. Blocking experiments, control studies with ^{64}Cu-DOTA-cetuximab, as well as ex vivo histology all confirmed the in vivo target specificity of ^{64}Cu-DOTA-TRC105.

Conclusion—This is the first successful PET imaging study of CD105 expression. Fast, prominent, persistent, and CD105-specific uptake of the tracer in the 4T1 tumour was observed. Further studies are warranted and currently underway.

[*]**Requests for reprints:** Weibo Cai, PhD, Departments of Radiology and Medical Physics, School of Medicine and Public Health, University of Wisconsin - Madison, 1111 Highland Ave, Room 7137, Madison, WI 53705-2275, USA, wcai@uwhealth.org; Phone: 608-262-1749; Fax: 608- 265-0614.
[6]Contributed equally to this work

Conflict of Interest

BRL is an employee of TRACON Pharmaceuticals, Inc. The other authors declare that they have no conflict of interest.

Keywords

CD105/Endoglin; Positron emission tomography (PET); Tumour angiogenesis; ^{64}Cu; RadioimmunoPET; TRC105

Introduction

Over the last decade, molecular imaging of angiogenesis has gained tremendous interest since angiogenesis is a fundamental process in both normal physiology and many disease processes such as tumour development and metastasis [1,2]. Two of the most intensively studied angiogenesis-related targets are integrin $\alpha_v\beta_3$ and vascular endothelial growth factor receptors (VEGFRs). Several tracers targeting these two receptors are already in clinical investigation [3-5]. Another attractive target related to tumour angiogenesis is CD105, also known as endoglin. CD105 is a disulphide-linked homodimeric transmembrane protein with a molecular weight of 180 kDa, composed of short intracellular and transmembrane domains and a large extracellular region [6,7].

CD105 is considered to be the most suitable marker for evaluating tumour angiogenesis [8,9]. Levels of CD105 expression in the endothelia within neoplastic tissues correlate with the proliferation rate of endothelial cells [10,11]. Studies have revealed that CD105 is overexpressed in vascular endothelial cells of tissues undergoing angiogenesis (e.g. tumours or regenerating/inflamed tissues) [10-12]. High CD105 expression also correlates with poor prognosis in more than 10 solid tumour types, consistent with the increased vascular proliferation rate required for rapidly proliferating cancers [13-15]. These findings support the role of CD105 as an optimal marker of tumour angiogenesis, underscoring its emerging clinical potential as a prognostic, diagnostic, and therapeutic vascular target in cancer.

CD105-targeted imaging agents could represent a new paradigm for the assessment of anti-angiogenic therapeutics, thereby facilitating the understanding of the role and expression profile of CD105 in angiogenesis-related diseases [13,15,16]. Molecular imaging techniques that have targeted CD105 include molecular magnetic resonance imaging [17], single-photon emission computed tomography (SPECT) [11,18,19], and ultrasound [20-22]. Another study investigated a ^{177}Lu-labeled anti-CD105 antibody for potential radioimmunotherapy applications [23]. All of these studies are based on conjugating various imaging or therapeutic labels (e.g., radioisotopes such as ^{111}In/^{99m}Tc/^{125}I/^{177}Lu, Gd-DTPA liposomes, or microbubbles) to anti-CD105 monoclonal antibodies (e.g. MAEND3, E9, and MJ7/18). To the best of our knowledge, positron emission tomography (PET) imaging of CD105 expression has not been previously studied. The excellent sensitivity, superb tissue penetration, and accurate quantification capability of PET warrant the development of a PET tracer for CD105 imaging in preclinical tumour models as well as for future clinical investigation.

TRC105 is a human/murine chimeric IgG1 monoclonal antibody which binds to both human and murine CD105 (with lower affinity to the latter) and inhibits angiogenesis and tumour growth. The murine parent antibody of TRC105 has been shown to induce apoptosis of human endothelial cells [24], mediate TGF-β-dependent inhibition of human endothelium [25], and inhibit the growth of syngeneic murine tumour grafts [26]. Compared with other anti-CD105 antibodies, TRC105 has a very high avidity (with a K_D of 2 ng/mL) for human CD105 and is currently in a multicenter Phase 1 first-in-human dose-escalation trial in the United States [27]. Multiple Phase 2 therapy trials are planned or underway in patients with various solid tumor types. In this study, we conjugated TRC105 with 1,4,7,10-

tetraazacyclododecane-1,4,7,10-tetraacetic acid (DOTA) and investigated the resulting DOTA-TRC105 conjugate both in vitro and in vivo.

Materials and methods

Reagents

TRC105 (a human/murine chimeric IgG1 monoclonal antibody which binds to CD105) was provided by TRACON pharmaceuticals Inc. (San Diego, CA). Cetuximab (a human/murine chimeric IgG1 monoclonal antibody that binds to human epidermal growth factor receptor [EGFR] but does not cross-react with the murine EGFR, http://www.accessdata.fda.gov/drugsatfda_docs/bla/2004/125084_ERBITUX_PHARMR_P1.PDF) was from Bristol-Meyers Squibb Company (Princeton, NJ). AlexaFluor488- and Cy3-labeled secondary antibodies were purchased from Jackson Immunoresearch Laboratories, Inc. (West Grove, CA). DOTA-NHS was purchased from Macrocyclics, Inc. (Dallas, TX) and Chelex 100 resin (50-100 mesh) was purchased from Sigma-Aldrich (St. Louis, MO). Water and all buffers were Millipore grade and pre-treated with Chelex 100 resin to ensure that the aqueous solution was heavy-metal free. PD-10 desalting columns were purchased from GE Healthcare (Piscataway, NJ). ^{64}Cu was produced via a ^{64}Ni(p,n)^{64}Cu reaction using a cyclotron at the University of Wisconsin-Madison.

Cell lines and animal model

4T1 murine breast cancer, MCF-7 human breast cancer, and human umbilical vein endothelial cells (HUVECs) were obtained from the American Type Culture Collection (ATCC, Manassas, VA). 4T1 and MCF-7 cells were cultured in RPMI 1640 medium (Invitrogen, Carlsbad, CA) with 10% fetal bovine serum and incubated at 37 °C with 5% CO_2. HUVECs were cultured in M-200 medium (Invitrogen, Carlsbad, CA) with 1× low serum growth supplement (Cascade Biologics, Portland, OR) and incubated at 37 °C with 5% CO_2. Cells were used for in vitro and in vivo experiments when they reached ~80% confluence.

All animal studies were conducted under a protocol approved by the University of Wisconsin Institutional Animal Care and Use Committee. For the 4T1 tumour model, four- to five-week-old female Balb/c mice were purchased from Harlan (Indianapolis, IN) and tumours were established by subcutaneously injecting 2×10^6 cells, suspended in 100 μL of 1:1 mixture of RPMI 1640 and matrigel (BD Biosciences, Franklin lakes, NJ), into the front flank of mice [28]. The tumour sizes were monitored every other day and the animals were subjected to in vivo experiments when the diameter of the tumours reached 6-8 mm (typically 7-10 days after inoculation).

DOTA conjugation and ^{64}Cu-labeling

Detailed procedures for DOTA conjugation have been reported previously [29,30]. DOTA-TRC105 and DOTA-cetuximab were purified using PD-10 columns and the final concentrations of DOTA-TRC105 and DOTA-cetuximab were measured based on UV absorbance at 280 nm using known concentrations of unconjugated TRC105 or cetuximab as the standard. For radiolabeling, $^{64}CuCl_2$ (74 MBq) was diluted in 300 μL of 0.1 M sodium acetate buffer (pH 6.5) and added to 50 μg of DOTA-TRC105 or DOTA-cetuximab. The reaction mixture was incubated for 30 min at 40 °C with constant shaking. ^{64}Cu-DOTA-TRC105 and ^{64}Cu-DOTA-cetuximab were purified using PD-10 columns with phosphate-buffered saline (PBS) as the mobile phase. The radioactive fractions containing ^{64}Cu-DOTA-TRC105 or ^{64}Cu-DOTA-cetuximab were collected and passed through a 0.2 μm syringe filter for in vivo experiments.

Flow cytometry and microscopy

The immunoreactivity of TRC105 and DOTA-TRC105 to HUVECs (high CD105 expression [11,31]) and MCF-7 (CD105-negative [11]) cells was evaluated by flow cytometry. Briefly, cells were harvested and suspended in cold PBS with 2% bovine serum albumin (BSA) at a concentration of 5×10^6 cells/ml. The cells were incubated with TRC105 or DOTA-TRC105 (1,5, or 10 μg/ml) for 30 min at room temperature (RT), washed three times with cold PBS, and centrifuged at 1000 rpm for 5 min. The cells were then incubated with AlexaFluor488-labeled goat anti-human IgG for 30 min at RT. Afterwards, the cells were washed and analyzed by flow cytometry using a BD FACSCalibur 4-color analysis cytometer equipped with 488nm and 633nm lasers (Becton-Dickinson, San Jose, CA) and FlowJo analysis software (Tree Star, Inc., Ashland, OR). HUVECs were also incubated with TRC105 or DOTA-TRC105 (2 μg/ml) and then examined under a Nikon Eclipse Ti microscope to further validate the FACS results.

MicroPET, microPET/microCT, and biodistribution studies

PET scans were performed using a microPET/microCT Inveon rodent model scanner (Siemens Medical Solutions USA, Inc.). Each tumour-bearing mouse was injected with 5-10 MBq of the PET tracer via tail vein and 3-15 min static PET scans were performed at various time points post injection (p.i.). The images were reconstructed using a maximum a posteriori (MAP) algorithm, with no attenuation or scatter correction. For each microPET scan, three-dimensional (3D) regions-of-interest (ROIs) were drawn over the tumour and major organs by using vendor software (Inveon Research Workshop; IRW) on decay-corrected whole-body images. Assuming a tissue density of 1 g/ml, the ROIs were converted to MBq/g using a conversion factor (pre-determined using a 50 ml centrifuge tube filled with $^{64}CuCl_2$ as a phantom), and then divided by the administered radioactivity to obtain an image ROI-derived percentage injected dose per gram of tissue (%ID/g). A 4T1 tumour-bearing mouse was injected with 2 mg of unlabeled TRC105 at 2 h earlier than ^{64}Cu-DOTA-TRC105 administration to evaluate the CD105 specificity of the tracer in vivo (i.e. blocking experiment). As an isotype-matched control, ^{64}Cu-DOTA-cetuximab (5-10 MBq) was intravenously injected into tumour-bearing mice and microPET scans were carried out as described above. After the PET scans, the mice were euthanized. The 4T1 tumour, liver, and spleen (tissues with high uptake of the tracer) were harvested for immunofluorescence staining.

To anatomically localize the tracer signal obtained using PET, a few animals were also subjected to microCT scans. Immediately after PET scanning, animals were transported to the microCT scanning gantry, positioned, and scanned at a voxel resolution of 97 μm (scanning time: 7 min). Fiducial markers were used for co-registration and images were reconstructed using the built-in software (Inveon Acquisition Workshop; Siemens). The microCT and microPET datasets were loaded into IRW and fiducial markers were co-registered for alignment of datasets.

Biodistribution studies were carried on a subset of animals to confirm that the quantitative tracer uptake values based on microPET imaging truly represented the actual tracer distribution in tumour-bearing mice. After the last PET scans at 48 h p.i., mice were euthanized and blood, 4T1 tumour, and major organs/tissues were collected and wet-weighed. The radioactivity in the tissue was measured using a gamma-counter (Perkin Elmer) and presented as %ID/g (mean ± SD).

Immunofluorescence staining

Frozen tissue slices (5 μm thickness) were fixed with cold acetone for 10 min and dried in the air for 30 min. After rinsing with PBS and blocking with 10% donkey serum for 30 min

at RT, the slices were incubated with TRC105 (2 μg/ml) for 1 h at 4 °C and visualized using AlexaFluor488-labeled goat anti-human secondary antibody. The tissue slices were also stained for endothelial marker CD31 (platelet/endothelial cell adhesion molecule; PECAM) as described previously [32]. After washing with PBS, the slides were incubated with rat anti-mouse CD31 antibody (2 μg/ml) for 1 h, followed by Cy3-labeled donkey anti-rat IgG for 30 min. All images were taken with a Nikon Eclipse Ti microscope.

Statistical analysis

Quantitative data were expressed as mean ± SD. Means were compared using Student's t-test. P values < 0.05 were considered statistically significant.

Results

In vitro investigation of DOTA-TRC105

As shown in Fig. 1, DOTA conjugation of TRC105 did not alter its CD105 binding affinity, as evidenced by both FACS analysis and fluorescence microscopy. In FACS analysis of HUVECs (which express a high level of CD105), there were no observable differences between TRC105 and DOTA-TRC105 at 1 μg/mL or 5 μg/mL (Fig. 1a). The binding to HUVECs was specific, as neither TRC105 nor DOTA-TRC105 bound to CD105-negative MCF-7 cells, even at a much higher concentration of 10 μg/mL (Fig. 1a). In addition to FACS analysis, fluorescence microscopy was also performed on HUVECs. No significant differences between TRC105 and DOTA-TRC105 were observed (Fig. 1b). Taken together, these in vitro studies confirmed that DOTA conjugation does not alter the antigen binding avidity or specificity of TRC105.

^{64}Cu-labeling

^{64}Cu-labeling including final purification using PD-10 columns took 80 ± 10 min (n = 10). The decay-corrected radiochemical yield was > 90% based on 25 μg of protein (DOTA-TRC105 or DOTA-cetuximab) per 37 MBq of ^{64}Cu, and the radiochemical purity was > 98%. The specific activity of both ^{64}Cu-DOTA-TRC105 and ^{64}Cu-DOTA-cetuximab was about 3.0 GBq/mg protein, assuming virtually complete recovery of the protein after size exclusion chromatography. Based on the specific activity of ^{64}Cu (~5% of the theoretical value of 254 Ci/μmol) and the amount of DOTA-TRC105 or DOTA-cetuximab used for radiolabeling, it was calculated that there were 0.42 ± 0.04 (n = 3) ^{64}Cu ions per antibody molecule (TRC105 or cetuximab).

MicroPET studies

Based on our previous studies with ^{64}Cu-labeled antibodies [29,30,33], the time points of 4, 24, and 48 h p.i. were chosen for serial PET scans after intravenous tracer injection. The coronal slices that contain tumours are shown in Fig. 2a and representative microPET/microCT fused images of a mouse at 24 h p.i. of ^{64}Cu-DOTA-TRC105 are shown in Fig. 2b. The quantitative data obtained from ROI analysis are shown in Fig. 2c&d. Consistent with our previous findings of radiolabeled antibodies, the uptake of ^{64}Cu-DOTA-TRC105 in the liver (due to hepatic clearance and some trans-chelation of ^{64}Cu) and blood pool (due to long circulation life-time of the antibody) was prominent at early time points and gradually declined over time. The liver uptake of ^{64}Cu-DOTA-TRC105 was 26.6 ± 2.2, 12.8 ± 0.7, and 9.6 ± 0.6 %ID/g at 4, 24, and 48 h p.i. respectively while the radioactivity in the blood was 16.5 ± 1.3, 8.0 ± 1.5, and 6.5 ± 1.4 %ID/g at 4, 24, and 48 h p.i. respectively (n = 3, Fig. 2c). The tumour uptake of ^{64}Cu-DOTA-TRC105 was clearly visible at 4 h p.i. and plateaued after 24 h p.i. (8.0 ± 0.5, 10.4 ± 2.8, and 9.7 ± 1.8 %ID/g at 4, 24, and 48 h p.i. respectively; n = 3; Fig. 2c&d), indicating antigen specific binding. Administrating a blocking dose of

TRC105 two hours before ^{64}Cu-DOTA-TRC105 injection reduced the tumour uptake to background level (Fig. 2a&d), which indicated CD105 specificity of the tracer in vivo.

To further investigate the CD105 specificity of ^{64}Cu-DOTA-TRC105, ^{64}Cu-DOTA-cetuximab was used as an isotype-matched control. Both TRC105 and cetuximab are human/murine chimeric IgG1 monoclonal antibodies. Since cetuximab does not cross-react with murine tissues, it serves as an excellent control for investigating the tracer uptake in the tumour due to passive targeting only (i.e. the enhanced permeability and retention effect). As can be seen in Fig. 2a&d, the uptake of ^{64}Cu-DOTA-cetuximab is at the background level (< 2.5 %ID/g) and significantly lower than that of ^{64}Cu-DOTA-TRC105 at all three time points examined ($P < 0.05$; $n = 3$), which further confirmed the CD105 specificity of ^{64}Cu-DOTA-TRC105 in vivo.

Biodistribution studies

After the last PET scans at 48 h p.i., the mice were euthanized. The tissues were collected for biodistribution and immunofluorescence staining studies to further validate the in vivo PET data. A separate group of three mice were injected with ^{64}Cu-DOTA-TRC105 and euthanized at 24 h p.i. for biodistribution studies (Fig. 3a). Besides the liver and spleen, the kidneys also had significant tracer uptake at 24 h p.i., however the absolute uptake was less than that of the 4T1 tumour. Tracer uptake in all other tissues was lower than the tumour. Comparing the biodistribution data at 24 h and 48 h p.i., uptake in most tissues dropped significantly yet the tumour uptake remained prominent with little decline, which was indicative of specific interactions between an antibody and its antigen. At 48 h p.i., the tumour uptake was higher than all major organs in the mice, thus providing good contrast. The tumour/muscle ratio was 22.1 ± 1.5 and 25.2 ± 1.2 at 24 h and 48 h p.i. respectively ($n = 3$).

A comparison of the biodistribution data of ^{64}Cu-DOTA-TRC105 and ^{64}Cu-DOTA-cetuximab at 48 h p.i. revealed that the uptake of ^{64}Cu-DOTA-cetuximab was higher in most organs except the 4T1 tumour (Fig. 3b), which again indicated the tumour specificity of ^{64}Cu-DOTA-TRC105. Overall, the quantification results obtained from biodistribution studies and PET scans matched very well, confirming that quantitative ROI analysis of non-invasive microPET scans truly reflected the distribution of PET tracers in vivo.

Histology

Immunofluorescence CD105/CD31 staining of various tissues ex vivo revealed that CD105 expression in the 4T1 tumour was primarily on the tumour vasculature, as evidenced by excellent co-localization of CD105 and CD31 staining and very weak signal on the 4T1 tumour cells (Fig. 4). CD105 staining of mouse liver and spleen both gave very low signal, indicating that these tissues do not have significant level of CD105 expression (Fig. 4). Therefore, tracer uptake in the liver and spleen was largely unrelated to CD105 binding and more likely related to non-specific capture by the reticuloendothelial system, hepatic clearance, and possibly trans-chelation of ^{64}Cu. Taken together, the ex vivo findings corroborated the in vivo data of ^{64}Cu-DOTA-TRC105, warranting further investigation of this tracer.

Discussion

The currently accepted standard method for quantifying angiogenesis is to assess MVD by performing CD105 immunohistochemistry on tumour tissue, an independent prognostic factor for survival in patients with many types of solid tumours [15,34,35]. CD105 has the advantage of being selectively expressed on proliferating endothelial cells at significantly

higher levels (up to 3×10^6 copies per cell) than other angiogenic targets like the VEGFRs (less than 0.2×10^6 copies per cell) [31]. Non-invasive imaging of CD105 expression has the potential to accelerate drug development by providing a reliable measure of angiogenesis in the entire body as an intact system, thereby facilitating individualized treatment monitoring and dose optimization in animal models, clinical trials, and ultimately in the day-to-day management of cancer patients. Therefore, the goal of this study was to develop a CD105-specific PET tracer. We have achieved this goal and investigated TRC105 and its conjugates in vitro, in vivo, and ex vivo.

The rationale for choosing the 4T1 tumour model for this study is that the parent antibody of TRC105 (SN6j, a monoclonal antibody of murine origin which binds to CD105) has been shown to be effective as an anti-angiogenic agent in this model [26]. Further, this is a rapidly growing tumour model. Thus it has highly angiogenic tumour vasculature (Fig. 4) which is expected to provide sufficient target density for imaging applications. One limitation of this model is that the tumour vasculature is of murine origin. TRC105 has significantly higher affinity to human CD105 than its murine homolog [36]. Thus, the 4T1 tumour model is not optimal for testing TRC105. Compared with other antibody-based PET tracers, tumour accumulation in this study is relatively low (~10 %ID/g). This is largely due to two facts: the tracer targets tumour vasculature but not tumour cells (there are fewer tumour vascular endothelial cells than tumour cells which are the target of most antibodies used for tumor imaging) and the sub-optimal affinity of TRC105 to murine endothelial cells relative to human endothelial cells. For future investigation, the following strategies may be adopted to better mimic the clinical situation: stably transfect 4T1 cells with human CD105, use transgenic mice with human tumour vasculature, or test an anti-CD105 antibody that binds with high affinity to murine CD105. Follow-up studies are currently underway. Nonetheless, excellent tumour contrast was achieved in this study, which justifies optimism that this tracer may perform better in cancer patients than we see here in mouse models of cancer.

The stability of radiometal-labeled antibody in vivo is always a concern. Many chelators have been investigated for ^{64}Cu-labeling and DOTA is one of the most intensively studied [37]. To confirm that the tumour uptake of ^{64}Cu-DOTA-TRC105 as observed in the in vivo studies was indeed antigen specific, various control experiments (e.g. blocking, an isotype-matched control) and in vitro/ex vivo experiments (e.g. FACS, microscopy, and histology) were performed to validate this aspect. We also plan to investigate other chelators (e.g. NOTA, TETA, among others) for ^{64}Cu-labeling in the future and compare the findings with the DOTA conjugates. One advantage of DOTA is that it is a universal chelator which can complex a wide variety of imaging and therapeutic radioisotopes. The same DOTA conjugate can therefore be employed for both imaging and therapeutic applications, with the use of appropriate radioisotopes, without affecting the pharmacokinetics and tumour targeting efficacy of the antibody conjugate.

One of the most interesting findings from this study was the difference between biodistribution patterns of ^{64}Cu-DOTA-TRC105 and ^{64}Cu-DOTA-cetuximab at 48 h p.i. The uptake of ^{64}Cu-DOTA-cetuximab is higher in most organs except the 4T1 tumour (Fig. 3b). Such an obvious difference between isotype-matched antibodies (both are human/murine chimeric IgG1 type) is likely due to the lack of cross-reactivity with murine tissues for cetuximab, which leads to longer circulation half-life and slower clearance/sequestration than TRC105 (which cross-reacts with murine CD105 although with lower affinity than human CD105). The overall charge of the two antibodies may also have played a role.

The advantages of antibody-based tracers are that they are quite antigen-specific and have high binding affinity and absolute tumour uptake, which makes them suitable for internal

radiotherapy applications and/or targeted delivery of drugs. To provide more insight about the long-term behavior of TRC105 in vivo, other longer lived isotopes (e.g. ^{89}Zr, ^{74}As, etc.) may be explored in future studies. The major limitations of antibody-based imaging are slow tumour accumulation and high background signal in the reticuloendothelial system, which may be overcome by peptide, small molecule, or antibody fragment-based tracers since they typically exhibit fast blood clearance. High-affinity CD105-binding peptides could be generated from various high-throughput screening strategies such as phage display. Anti-CD105 antibody fragments, both human and murine [38,39], as well as certain bi-specific antibodies [40,41], may also be investigated in the future for imaging and potential therapeutic applications. Lastly, quantitative correlation of PET tracer uptake with CD105 expression level would be highly desirable for future treatment monitoring applications, as it would be ideal to non-invasively measure the changes of CD105 expression quantitatively, rather than qualitatively, in each individual patient upon anti-angiogenic therapies.

Conclusion

We have successfully investigated ^{64}Cu-DOTA-TRC105, a human-murine chimeric antibody recognizing both human and murine CD105, both in vitro and in vivo. MicroPET imaging revealed fast, prominent, persistent, and CD105-specific uptake of the tracer in the 4T1 tumour which was further validated by in vitro and ex vivo experiments. Since TRC105 is already in clinical investigation and therapeutic efficacy has been shown in various animal tumour models and certain cancer patients, this study identifies a new perspective for tumour angiogenesis-related research and warrants future clinical translation of ^{64}Cu-DOTA-TRC105, where it may be used to evaluate the pharmacokinetics, tumour targeting efficacy, dose optimization, and dose interval of TRC105 and TRC105-based cancer therapeutics in the clinic.

Acknowledgments

This work is supported, in part, by the Wisconsin Partnership Program, the University of Wisconsin Carbone Cancer Center, NCRR 1UL1RR025011, a Susan G. Komen Postdoctoral Fellowship (to H. Hong), and a DOD PCRP IDEA Award.

References

1. Carmeliet P. Angiogenesis in life, disease and medicine. Nature. 2005; 438:932–6. [PubMed: 16355210]
2. Folkman J. Angiogenesis in cancer, vascular, rheumatoid and other disease. Nat Med. 1995; 1:27–31. [PubMed: 7584949]
3. Cai W, Chen X. Multimodality imaging of vascular endothelial growth factor and vascular endothelial growth factor receptor expression. Front Biosci. 2007; 12:4267–79. [PubMed: 17485373]
4. Cai W, Niu G, Chen X. Imaging of integrins as biomarkers for tumor angiogenesis. Curr Pharm Des. 2008; 14:2943–73. [PubMed: 18991712]
5. Dijkgraaf I, Boerman OC. Radionuclide imaging of tumor angiogenesis. Cancer Biother Radiopharm. 2009; 24:637–47. [PubMed: 20025543]
6. Barbara NP, Wrana JL, Letarte M. Endoglin is an accessory protein that interacts with the signaling receptor complex of multiple members of the transforming growth factor-beta superfamily. J Biol Chem. 1999; 274:584–94. [PubMed: 9872992]
7. Gougos A, Letarte M. Primary structure of endoglin, an RGD-containing glycoprotein of human endothelial cells. J Biol Chem. 1990; 265:8361–4. [PubMed: 1692830]
8. Fonsatti E, Del Vecchio L, Altomonte M, Sigalotti L, Nicotra MR, Coral S, et al. Endoglin: An accessory component of the TGF-beta-binding receptor-complex with diagnostic, prognostic, and

bioimmunotherapeutic potential in human malignancies. J Cell Physiol. 2001; 188:1–7. [PubMed: 11382917]

9. Wang JM, Kumar S, Pye D, van Agthoven AJ, Krupinski J, Hunter RD. A monoclonal antibody detects heterogeneity in vascular endothelium of tumours and normal tissues. Int J Cancer. 1993; 54:363–70. [PubMed: 8509210]
10. Burrows FJ, Derbyshire EJ, Tazzari PL, Amlot P, Gazdar AF, King SW, et al. Up-regulation of endoglin on vascular endothelial cells in human solid tumors: implications for diagnosis and therapy. Clin Cancer Res. 1995; 1:1623–34. [PubMed: 9815965]
11. Fonsatti E, Jekunen AP, Kairemo KJ, Coral S, Snellman M, Nicotra MR, et al. Endoglin is a suitable target for efficient imaging of solid tumors: in vivo evidence in a canine mammary carcinoma model. Clin Cancer Res. 2000; 6:2037–43. [PubMed: 10815930]
12. Wikstrom P, Lissbrant IF, Stattin P, Egevad L, Bergh A. Endoglin (CD105) is expressed on immature blood vessels and is a marker for survival in prostate cancer. Prostate. 2002; 51:268–75. [PubMed: 11987155]
13. Dallas NA, Samuel S, Xia L, Fan F, Gray MJ, Lim SJ, et al. Endoglin (CD105): a marker of tumor vasculature and potential target for therapy. Clin Cancer Res. 2008; 14:1931–7. [PubMed: 18381930]
14. Kumar S, Ghellal A, Li C, Byrne G, Haboubi N, Wang JM, et al. Breast carcinoma: vascular density determined using CD105 antibody correlates with tumor prognosis. Cancer Res. 1999; 59:856–61. [PubMed: 10029075]
15. Fonsatti E, Nicolay HJ, Altomonte M, Covre A, Maio M. Targeting cancer vasculature via endoglin/CD105: a novel antibody-based diagnostic and therapeutic strategy in solid tumours. Cardiovasc Res. 86:12–9. [PubMed: 19812043]
16. Cai W, Rao J, Gambhir SS, Chen X. How molecular imaging is speeding up antiangiogenic drug development. Mol Cancer Ther. 2006; 5:2624–33. [PubMed: 17121909]
17. Zhang D, Feng XY, Henning TD, Wen L, Lu WY, Pan H, et al. MR imaging of tumor angiogenesis using sterically stabilized Gd-DTPA liposomes targeted to CD105. Eur J Radiol. 2009; 70:180–9. [PubMed: 18541399]
18. Bredow S, Lewin M, Hofmann B, Marecos E, Weissleder R. Imaging of tumour neovasculature by targeting the TGF-beta binding receptor endoglin. Eur J Cancer. 2000; 36:675–81. [PubMed: 10738134]
19. Costello B, Li C, Duff S, Butterworth D, Khan A, Perkins M, et al. Perfusion of ^{99m}Tc-labeled CD105 Mab into kidneys from patients with renal carcinoma suggests that CD105 is a promising vascular target. Int J Cancer. 2004; 109:436–41. [PubMed: 14961584]
20. Korpanty G, Carbon JG, Grayburn PA, Fleming JB, Brekken RA. Monitoring response to anticancer therapy by targeting microbubbles to tumor vasculature. Clin Cancer Res. 2007; 13:323–30. [PubMed: 17200371]
21. Korpanty G, Grayburn PA, Shohet RV, Brekken RA. Targeting vascular endothelium with avidin microbubbles. Ultrasound Med Biol. 2005; 31:1279–83. [PubMed: 16176794]
22. Cui S, Lu SZ, Chen YD, He GX, Liu JP, Song ZY, et al. Relationship between intravascular ultrasound imaging features of coronary plaques and soluble CD105 level in patients with coronary heart disease. Chin Med J (Engl). 2007; 120:595–7. [PubMed: 17442209]
23. Lee SY, Hong YD, Felipe PM, Pyun MS, Choi SJ. Radiolabeling of monoclonal anti-CD105 with ^{177}Lu for potential use in radioimmunotherapy. Appl Radiat Isot. 2009; 67:1366–9. [PubMed: 19324561]
24. Tsujie M, Tsujie T, Toi H, Uneda S, Shiozaki K, Tsai H, et al. Anti-tumor activity of an anti-endoglin monoclonal antibody is enhanced in immunocompetent mice. Int J Cancer. 2008; 122:2266–73. [PubMed: 18224682]
25. She X, Matsuno F, Harada N, Tsai H, Seon BK. Synergy between anti-endoglin (CD105) monoclonal antibodies and TGF-beta in suppression of growth of human endothelial cells. Int J Cancer. 2004; 108:251–7. [PubMed: 14639611]
26. Tsujie M, Uneda S, Tsai H, Seon BK. Effective anti-angiogenic therapy of established tumors in mice by naked anti-human endoglin (CD105) antibody: differences in growth rate and therapeutic

response between tumors growing at different sites. Int J Oncol. 2006; 29:1087–94. [PubMed: 17016638]

27. Mendelson DS, Gordon MS, Rosen LS, Hurwitz H, Wong MK, Adams BJ, et al. Phase I study of TRC105 (anti-CD105 [endoglin] antibody) therapy in patients with advanced refractory cancer. J Clin Oncol. 2010; 28:15s.
28. Wang H, Cai W, Chen K, Li ZB, Kashefi A, He L, et al. A new PET tracer specific for vascular endothelial growth factor receptor 2. Eur J Nucl Med Mol Imaging. 2007; 34:2001–10. [PubMed: 17694307]
29. Cai W, Chen K, He L, Cao Q, Koong A, Chen X. Quantitative PET of EGFR expression in xenograft-bearing mice using ^{64}Cu-labeled cetuximab, a chimeric anti-EGFR monoclonal antibody. Eur J Nucl Med Mol Imaging. 2007; 34:850–58. [PubMed: 17262214]
30. Cai W, Wu Y, Chen K, Cao Q, Tice DA, Chen X. *In vitro* and *in vivo* characterization of ^{64}Cu-labeled Abegrin™, a humanized monoclonal antibody against integrin $\alpha_v\beta_3$. Cancer Res. 2006; 66:9673–81. [PubMed: 17018625]
31. Takahashi N, Haba A, Matsuno F, Seon BK. Antiangiogenic therapy of established tumors in human skin/severe combined immunodeficiency mouse chimeras by anti-endoglin (CD105) monoclonal antibodies, and synergy between anti-endoglin antibody and cyclophosphamide. Cancer Res. 2001; 61:7846–54. [PubMed: 11691802]
32. Cai W, Chen K, Mohamedali KA, Cao Q, Gambhir SS, Rosenblum MG, et al. PET of vascular endothelial growth factor receptor expression. J Nucl Med. 2006; 47:2048–56. [PubMed: 17138749]
33. Cai W, Ebrahimnejad A, Chen K, Cao Q, Li ZB, Tice DA, et al. Quantitative radioimmunoPET imaging of EphA2 in tumor-bearing mice. Eur J Nucl Med Mol Imaging. 2007; 34:2024–36. [PubMed: 17673999]
34. Duff SE, Li C, Garland JM, Kumar S. CD105 is important for angiogenesis: evidence and potential applications. FASEB J. 2003; 17:984–92. [PubMed: 12773481]
35. Fonsatti E, Sigalotti L, Arslan P, Altomonte M, Maio M. Emerging role of endoglin (CD105) as a marker of angiogenesis with clinical potential in human malignancies. Curr Cancer Drug Targets. 2003; 3:427–32. [PubMed: 14683500]
36. Matsuno F, Haruta Y, Kondo M, Tsai H, Barcos M, Seon BK. Induction of lasting complete regression of preformed distinct solid tumors by targeting the tumor vasculature using two new anti-endoglin monoclonal antibodies. Clin Cancer Res. 1999; 5:371–82. [PubMed: 10037187]
37. Wadas TJ, Wong EH, Weisman GR, Anderson CJ. Coordinating radiometals of copper, gallium, indium, yttrium, and zirconium for PET and SPECT imaging of disease. Chem Rev. 110:2858–902. [PubMed: 20415480]
38. Volkel T, Holig P, Merdan T, Muller R, Kontermann RE. Targeting of immunoliposomes to endothelial cells using a single-chain Fv fragment directed against human endoglin (CD105). Biochim Biophys Acta. 2004; 1663:158–66. [PubMed: 15157618]
39. Muller D, Trunk G, Sichelstiel A, Zettlitz KA, Quintanilla M, Kontermann RE. Murine endoglin-specific single-chain Fv fragments for the analysis of vascular targeting strategies in mice. J Immunol Methods. 2008; 339:90–8. [PubMed: 18790696]
40. Nettelbeck DM, Miller DW, Jerome V, Zuzarte M, Watkins SJ, Hawkins RE, et al. Targeting of adenovirus to endothelial cells by a bispecific single-chain diabody directed against the adenovirus fiber knob domain and human endoglin (CD105). Mol Ther. 2001; 3:882–91. [PubMed: 11407902]
41. Korn T, Muller R, Kontermann RE. Bispecific single-chain diabody-mediated killing of endoglin-positive endothelial cells by cytotoxic T lymphocytes. J Immunother. 2004; 27:99–106. [PubMed: 14770081]

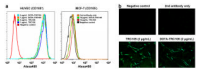

Fig. 1.

In vitro investigation of DOTA-TRC105. **a** Flow cytometry analysis of TRC105 and DOTA-TRC105 in HUVECs (CD105-positive) and MCF-7 (CD105-negative) cells at different concentrations. **b** Fluorescence microscopy images of HUVECs using either TRC105 or DOTA-TRC105 (2 μg/mL) as the primary antibody. Various control images are also shown.

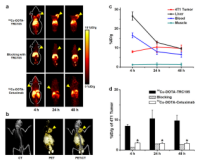

Fig. 2.

In vivo investigation of ^{64}Cu-DOTA-TRC105 in 4T1 tumour-bearing mice. **a** Serial coronal PET images of 4T1 tumour-bearing mice at 4, 24, and 48 h post-injection of ^{64}Cu-DOTA-TRC105, TRC105 before ^{64}Cu-DOTA-TRC105 (i.e. blocking), and ^{64}Cu-DOTA-cetuximab. Tumors are indicated by arrowheads. **b** Representative PET/CT images of ^{64}Cu-DOTA-TRC105 in 4T1 tumour-bearing mice at 24 h post-injection. **c** Time-activity curves of the tumour, liver, blood, and muscle upon intravenous injection of ^{64}Cu-DOTA-TRC105 into 4T1 tumour-bearing mice (n = 3). **d** Comparison of 4T1 tumour uptake of ^{64}Cu-DOTA-TRC105, ^{64}Cu-DOTA-TRC105 with a blocking does of TRC105, and ^{64}Cu-DOTA-cetuximab. *: $P < 0.05$ (n = 3).

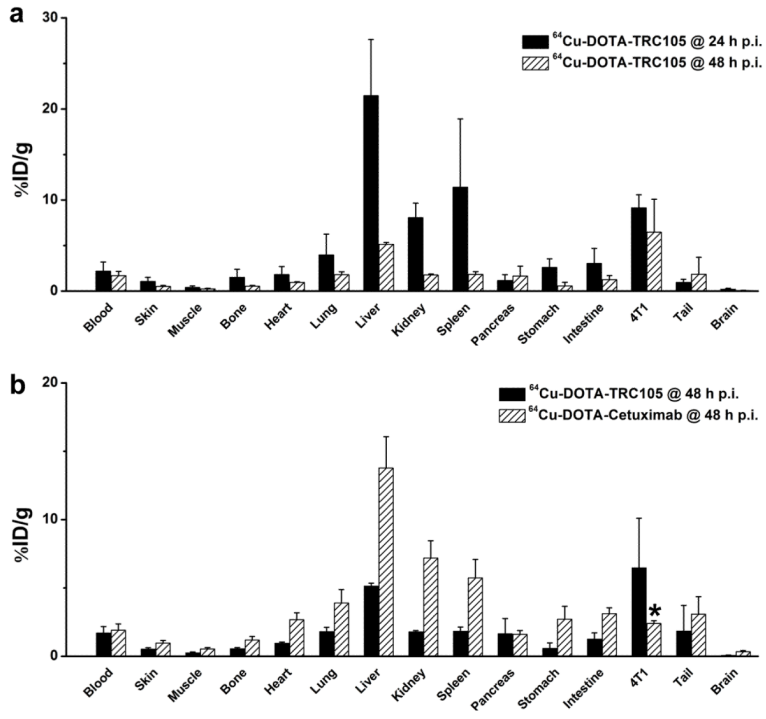

Fig. 3.

Biodistribution studies after non-invasive PET scans. **a** Biodistribution of ^{64}Cu-DOTA-TRC105 in 4T1 tumour-bearing mice at 24 and 48 h post-injection (n = 3). **b** Biodistribution of ^{64}Cu-DOTA-TRC105 and ^{64}Cu-DOTA-cetuximab at 48 h post-injection (n = 3). *: $P < 0.05$.

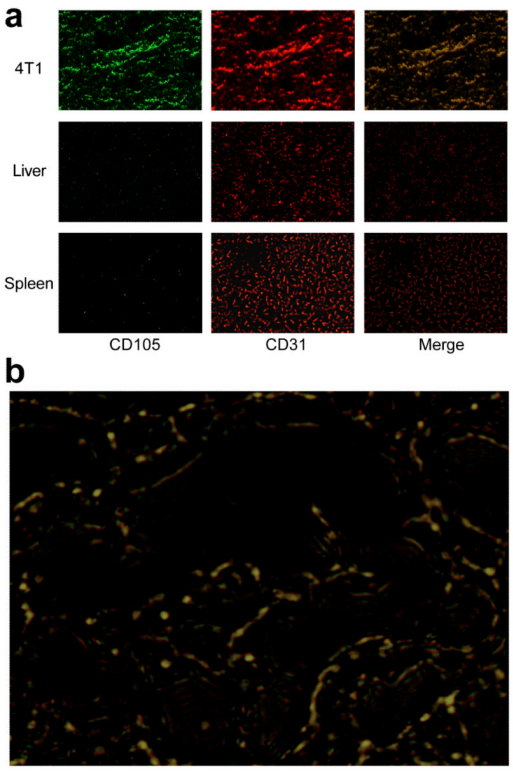

Fig. 4.

Immunofluorescence CD105/CD31 double-staining of the 4T1 tumour, liver, and spleen tissue sections. **a** TRC105 and AlexaFluor488-labeled goat anti-human IgG was used for CD105 staining (green). Afterwards, the tissue slices were stained with rat anti-mouse CD31 antibody and Cy3-labeled donkey anti-rat IgG (red). **b** A higher magnification merged image revealed that CD105 expression in the 4T1 tumour was almost exclusively on the vessels, evidenced by almost perfect overlay of the CD105 and CD31 staining.